Physical and Conformational Properties of Synthetic Idealized Signal Sequences Parallel Their Biological Function†

Jennifer W. Izard,‡ Michael B. Doughty,§ and Debra A. Kendall*,‡

The Department of Molecular and Cell Biology, The University of Connecticut, Storrs, Connecticut 06269, and The Department of Medicinal Chemistry, School of Pharmacy, The University of Kansas, Lawrence, Kansas 66045

Received March 23, 1995; Revised Manuscript Received June 2, 1995⊗

ABSTRACT: Transported proteins often contain an extension sequence called the signal peptide. The alkaline phosphatase (PhoA) signal sequence represents a typical signal peptide for comparison to idealized sequences both *in vivo* and *in vitro*. We have designed a series of idealized signal sequences which vary in amino terminal charge and core region hydrophobicity with minimal variation in amino acid composition. The idealized core regions contain different proportions of leucine and alanine residues, effectively producing hydrophobicities above and below the threshold level required for efficient secretion. The flanking amino and carboxyl termini were designed to maintain the general features and relative hydrophobicity of their counterparts in the wild-type PhoA signal sequence. Using the *phoA* gene, the signal peptide region was modified to generate mutants corresponding to the model sequences. Transport studies in *Escherichia coli* confirmed that completely idealized signal sequences, which lack a helix-breaking proline or glycine residue, can be functional if the core region is sufficiently hydrophobic and that one positively charged residue in the amino terminus is adequate for efficient transport. The corresponding peptides were chemically synthesized and exhibited HPLC retention times that reflect the relative hydrophobicities of the sequences. Structural analyses of the isolated peptides by circular dichroism demonstrate solvent dependence and exceptionally stable α-helix formation by the functional signal peptides in trifluoroethanol. Although leucine and alanine residues are often predicted to have similar propensities for forming an α-helix, considerably higher α-helical content is observed in the signal peptides which contain predominantly polyleucine core regions. This strong helical potential of leucine in the context of the signal peptide may be related to the especially efficient protein transport of polyleucine core region mutants [Rusch, S. L., Chen, H., Izard, J. W., & Kendall, D. A. (1994) *J. Cell. Biochem. 55*, 209−217].

Transported proteins in both prokaryotes and eukaryotes are often synthesized with an amino-terminal extension called the signal peptide or leader sequence. This sequence is responsible for targeting a protein for export via a secretory pathway and is usually removed upon membrane translocation by the signal peptidase enzyme. Interestingly, despite their common purpose, signal peptides have diverse primary sequences. However, they do exhibit common physical characteristics. The shared properties include a positively charged amino terminus, a highly hydrophobic core region, and a more polar carboxyl terminus with small side-chain amino acid residues in the −1 and −3 positions. Although these general characteristics have been determined [for review, see Izard and Kendall (1994)], the role that these play is not clearly defined and the interactions of signal peptides with the export machinery are not established.

The importance of the net positive charge in the amino terminus has been verified in several mutational studies, which have demonstrated a loss of transport efficiency in the absence of the positive charge [for example, Vlasuk et al. (1983)]. One study demonstrated that the extent of cross-linking of a precursor to purified SecA, a vital secretory component, was proportional to the number of positively charged residues in the amino terminus of the signal sequence (Akita et al., 1990). In addition, a secretion deficiency caused by lowering the charge at the amino terminus can be partially suppressed by mutants in the *prlD* (SecA) gene (Puziss et al., 1989). Alternatively, the significance of the net positive charge at the amino terminus is often attributed to an electrostatic attraction to the negatively charged phospholipid headgroups on the inner membrane [for review, see de Vrije et al. (1990)].

The hydrophobic residues in the core region tend to have substantial α-helical forming propensity (Austen, 1979), a conformation that would further enhance the overall hydrophobicity of this region. Although biophysical studies suggest that synthetic wild-type signal peptides adopt β-sheet or random structures in aqueous solutions, they can form α-helices in structure-promoting solvents such as TFE[1] and SDS [for review, see Gierasch (1989)]. In addition, the stability of the helix observed in synthetic LamB and OmpA mutant sequences has been correlated with their ability to

† This research was supported by grants from the National Institutes of Health (GM37639 to D.A.K.) and the Connecticut Department of Economic Development (93K024 to D.A.K.).

* Corresponding author. Phone: (203) 486-1891. Fax: (203) 486-1784. E-mail: kendall@uconnvm.uconn.edu.

‡ The University of Connecticut.

§ The University of Kansas.

⊗ Abstract published in *Advance ACS Abstracts,* July 15, 1995.

[1] Abbreviations: PhoA, alkaline phosphatase; TFE, 2,2,2-trifluoroethanol; SDS, sodium dodecyl sulfate; LB, Luria broth; MOPS, 4-morpholinepropanesulfonic acid; PCR, polymerase chain reaction; TCA, trichloroacetic acid; Tris, tris-(hydroxymethyl)aminomethane; EDTA, ethylenediaminetetraacetic acid; TFA, trifluoroacetic acid; HPLC, high-performance liquid chromatography; WT, wild type; FAB$^+$ MS, positive fast-atom bombardment mass spectrometry; PITC, phenylisothiocyanate; CD, circular dichroism; CCCP, carbonyl cyanide 3-chlorophenylhydrazone.

0006-2960/95/0434-9904$09.00/0

function *in vivo* (Bruch & Gierasch, 1990; Rizo et al., 1993). A highly hydrophobic α-helical structure could have functional implications as a recognition element, yet it is undeniably suitable for direct insertion into the lipid bilayer. It has also been suggested that the hydrophobic nature of the signal peptide may help the precursor protein to maintain a transport competent state (Park et al., 1988).

The carboxyl terminus is ideally six residues long and contains several polar amino acids which may serve to clearly demarcate the end of the core region, promoting efficient alignment of the cleavage site with the signal peptidase enzyme. The frequent appearance of a glycine or proline residue near the carboxyl end of the core region may also serve this purpose. It is well established that the signal peptidase will not accept bulky residues in the −1 and −3 positions (von Heijne, 1984; Laforet & Kendall, 1991).

In order to correlate function with physical properties, it has been instrumental to idealize specific segments of the alkaline phosphatase signal peptide for *in vivo* analysis. This approach involves eliminating some of the variables of natural signal sequences by replacing regions with polymers of only one or a few different amino acid residues (Kendall et al., 1986). In this way, we have demonstrated that function is dependent on overall physical properties rather than specific primary sequence and the limits of hydrophobicity and length in both the core and cleavage regions have been defined [for review, see Izard and Kendall (1994)]. In this study, we have designed a series of completely idealized signal sequences which systematically vary in amino terminal positive charge and core region hydrophobicity. The amino termini contain either one or three positively charged residues, and the core regions consist of different ratios of leucine to alanine residues producing net hydrophobicities above and below the threshold required for efficient export (Doud et al., 1993). These signal peptides are evaluated *in vivo* and, by the criteria examined, show no difference in transport activity with respect to the charge at the amino terminus but do show differences due to the composition of the core. The physical basis for this difference is examined by characterizing the corresponding synthetic peptides with regard to the parameters of hydrophobicity and conformation. According to predictions based on frequency in α-helices in natural proteins (Chou & Fasman, 1978; Munoz & Serrano, 1994) and on theoretical and biophysical studies (Lyu et al., 1990; O'Neil & DeGrado, 1990; Padmanabhan et al., 1990; Creamer & Rose, 1992) of model peptides, the α-helical preferences of leucine and alanine residues are similar. However, when the frequency of residues at various locations within helical segments is determined, leucine is clearly more prominent than alanine at internal positions (Chou & Fasman, 1974). Indeed, structural analyses of polymers of these residues in the context of idealized signal sequences reveal a substantial difference in structure that is dependent on solvent as well as the ratio of leucine to alanine residues in the core region. Furthermore, the high helical content of the polyleucine sequences in TFE may explain their unique transport properties observed in earlier studies (Rusch et al., 1994).

MATERIALS AND METHODS

Materials. Protected, N^{α}-Fmoc amino acids and all solvents used for peptide synthesis were purchased from ABI (currently Perkin Elmer Applied Biosystems Division, Foster City, CA). Ultra Pure SDS was purchased from Life Technologies, Inc. (Gaithersburg, MD). NMR grade TFE was purchased from Aldrich Chemical Co. (Milwaukee, WI).

Bacterial Strains and Media. Escherichia coli strain AW1043 (Δ*lac galU galK* Δ(*leu-ara*) *phoA-E15 proC*::Tn5) was used in all experiments. For general propagation of cells and for generation of mutants, bacteria were grown in LB medium (Miller, 1972) containing 250 μg/mL ampicillin and 50 μg/mL kanamycin. Transport studies were carried out in MOPS low phosphate (100 μM KH_2PO_4) medium (Neidhardt et al., 1974) which induces alkaline phosphatase expression.

Construction of Mutants. All of the mutants were produced by cassette mutagenesis using a newly generated plasmid, WT-Afl, a pBR322-PhoA derivative of WT-XN (Laforet & Kendall, 1991). This plasmid was created by using PCR to introduce a unique *Afl*II site just upstream of the initial methionine: the DNA sequence ATAAAG was changed to CTTAAG. The presence of this new restriction site, in addition to the *Bss*HII site, allows the removal of the entire signal peptide for replacement with completely idealized signal peptides. The vector was prepared for cassette insertion by digestion with *Afl*II and *Bss*HII and agarose gel electrophoresis to remove the DNA coding for the wild-type signal sequence. Synthetic oligonucleotides coding for the mutant signal peptide sequences were then annealed and ligated to the remaining vector. Each insert involved two pairs of complementary oligonucleotide strands; mutants containing the same core regions could be generated using the same pair of oligonucleotides coding for the carboxy-terminal end of the signal peptide. The oligonucleotides maintained the same codon usage for the core regions as in the design of the 8A2Lh and 3A7Lh mutants (Doud et al., 1993), and codon repetition in the amino terminal and cleavage regions was minimized. The mutant sequences were confirmed by restriction enzyme analysis and direct DNA sequencing (Sanger et al., 1977).

Pulse−Chase Analysis. To determine the rate of precursor processing, cells in the logarithmic growth phase were washed and resuspended in MOPS no phosphate medium supplemented with 20 μg/mL amino acids minus methionine. The cells were labeled at 37 °C with 40 μCi of L-[^{35}S]-methionine for 40 s and then chased with 4 mg/mL non-radioactive methionine for 30 s, 1 min, 5 min, and 20 min. Cells were precipitated with 10% TCA, the pellets were washed twice with ice-cold acetone, and alkaline phosphatase was immunoprecipitated as described previously (Kendall et al., 1986). After separation of the precursor and mature species on 7.5% Laemmli gels (Laemmli, 1970), the corresponding areas of dried gel, visualized by autoradiography, were excised and rehydrated. The radioactivity was solubilized from the gel matrix in 1 mL of 50% SOLVABLE (Du Pont NEN Research Products, Boston, MA) with gentle shaking at 55 °C for 3 h. Following incubation for 16−20 h in 10 mL of scintillation fluid at room temperature, the radioactivity was determined. The percentage of mature alkaline phosphatase for each sample was calculated, correcting for the additional radioactive methionine in the precursor form.

Cell Fractionation. Cells were grown and labeled as above, except that the labeling time was 60 s. Radiolabeled cells were removed to ice, and whole cell fractions were

immediately precipitated with 10% TCA. Periplasmic fractions were resuspended in 0.1 M Tris (pH 8.2), 0.5 M sucrose, and 0.5 mM EDTA. After a 5 min incubation on ice, freshly prepared lysozyme was added to a final concentration of about 80 μg/mL. Within 10−30 s, ice-cold water was added. The addition of 15 mM $MgCl_2$ stabilizes the formation of spheroplasts during a 5 min incubation on ice (Randall & Hardy, 1986). Cells were centrifuged, and the supernatant containing the periplasm was precipitated with 10% TCA. Alkaline phosphatase was immunoprecipitated from the whole cell and periplasmic fractions derived from equal amounts of cells.

Peptide Synthesis and Purification. Peptides were synthesized on Rink's resin (Fisher Scientific, Pittsburgh, PA) using an ABI Model 431A automated peptide synthesizer (facilities provided by The University of Connecticut Biotechnology Center) with FastMoc chemistry at a 0.1 mmol scale. The resin was loaded with cysteine as the first amino acid using a typical coupling cycle, and unreacted sites were capped with acetic anhydride. All subsequent amino acids were coupled using standard chemistry, protocols, and procedures supplied by the manufacturer. For peptides containing seven leucines in the core, amino acids in the hydrophobic segment were double coupled. Coupling efficiencies were typically followed by the quantitative ninhydrin test yielding coupling efficiencies ranging from 95% to 99%. After synthesis, the peptides were cleaved from the resin and fully deprotected by treatment with TFA containing 5% water with 5% thioanisole, 5% ethyl methyl sulfide, 2.5% ethanedithiol, and 7.5% phenol as scavengers for 1.5 h at 25 °C. Each peptide amide was then precipitated by the addition of an excess of *tert*-butyl methyl ether, and, after collection by centrifugation, the solid was dissolved in 0.1% aqueous TFA and lyophilized to dryness.

The crude peptides obtained from TFA cleavage were then subjected to a one-step purification using either isocratic or gradient reverse-phase HPLC. Peptides were chromatographed from a 1 × 25 cm Vydac C-4 semi-prep column at 3.0 mL/min using a Beckman System Gold HPLC with detection at 220 nm. Peptides WT, 3K2L, 1K2L, and 3K7L were eluted with 34%, 17%, 21%, and 39% acetonitrile in 0.1% TFA. Peptide 1K7L was purified by a shallow gradient from 30 to 50% acetonitrile in 0.1% TFA over 13 min.

The purified peptides were analyzed for purity and identity by analytical HPLC, amino acid analysis and FAB^+ MS. The retention times and purity of each peptide was ascertained using gradient elution from an analytical Vydac C-4 column (0.46 × 25 cm) eluting with 0−60% acetonitrile in 0.1% TFA with detection at 220 nm. Amino acid analysis was performed after hydrolysis in 6 N HCl containing 0.2% phenol at 115 °C under vacuum. Peptides WT and 3K2L were analyzed using precolumn PITC derivitization and a Waters (division of Millipore, Millford, MA) PicoTag amino acid hydrolysate analysis system at 38 °C. Peptides 1K2L, 3K7L, and 1K7L were analyzed by the W. M. Keck Foundation Biotechnology Resource Laboratory at Yale University (New Haven, CT) using a Beckman 7300 amino acid analyzer with ion-exchange separation and ninhydrin postcolumn derivitization. The FAB^+ MS analysis was performed on an AUTOSPEC-Q (Fisions VG, Ltd, Manchester, UK) equipped with a 35 keV cesium gun; the analysis was performed by voltage scanning over the mass range of 2000−2500.

Circular Dichroism Studies. CD spectra were recorded on an AVIV 60DS (WT and peptide 3K2L) or Jasco J-710 (peptides WT, 1K2L, 3K7L, 1K7L) spectropolarimeter standardized with (1*S*)-(+)-10-camphorsulfonic acid. Purified peptides were initially dissolved in deionized water and diluted into solutions of SDS (1 and 10 mM) or TFE (10, 20, or 40%). The stock peptide concentration was determined using the quantitative ninhydrin test of Moore and Stein (1954). CD measurements were carried out at 25 °C using siliconized CD cells. The results of CD experiments are expressed as mean residue molar ellipticity as calculated using

$$[\theta] = \mathrm{mD}\frac{1}{\mathrm{PL\#C}} \qquad (1)$$

where $[\theta]$ is the mean residue molar ellipticity in degree cm^2/dmol, mD is the CD signal in millidegrees, PL is the pathlength of the CD cell used in millimeters (mm), # is the number of residues in the peptide, and C is the total peptide concentration in moles per liter (M). CD spectra of peptides were taken in wavelength mode from 190 to 250 nm with a scan step size of 0.2, 0.5, or 1.0 nm. All CD spectra were baseline corrected. The secondary structural properties of peptides under these conditions were determined from the shape and intensity of the CD spectra as calculated by the method of Greenfield and Fasman (1969). For the CD spectrum that was outside of the extrema of the reference spectra used by Greenfield and Fasman, we additionally estimated helical content from $[\phi]_{222}$ by the method of Chen et al. (1974). Secondary structure estimation programs that use proteins for reference spectra were unable to adequately reproduce the shapes and intensities of all the CD spectra of these peptides.

RESULTS

Design of Idealized Signal Sequences. Numerous studies in our laboratory have demonstrated that global changes in signal peptide amino acid composition can be made without disrupting its function provided that the prominent physical characteristics are retained (Kendall et al., 1986; Laforet & Kendall, 1991). The wild-type alkaline phosphatase signal sequence is an example of a typical prokaryotic signal peptide, and it serves as a prototype for designing idealized signal sequences. Thus, the idealized sequences presented in Figure 1 retain the lengths of the three regions of this natural signal peptide. The model peptides also maintain the approximate hydrophobicity of the amino and carboxyl termini as well as that of the core region when a functional signal sequence was desired.

The aim in designing this series of idealized signal peptides is to facilitate clear comparisons between sequences with regard to changes in charge, hydrophobicity, and structural propensity with minimal changes in amino acid composition. The series consists of four peptides with combinations of two different amino termini, two different core regions, and a unique idealized cleavage region. The amino termini possess either one or three positively charged lysine residues, the basic amino acid most frequently found in this region. The initiating methionine was retained, and glutamine was chosen as a spacer in the amino terminus due to its polarity, neutral charge, and indifference as an amino-terminal helix capping residue (Forood et al., 1993). The selected core

FIGURE 1: Sequences of plasmid DNA and synthetic signal peptides. (A) The WT-Afl vector contains unique *Afl*II, *Sal*I, and *Bss*HII sites in the wild-type alkaline phosphatase structural gene. The *Afl*II site was introduced as described in Materials and Methods, and the residues that were altered are underlined. The arrow marks the position of signal peptidase cleavage. Amino acids are numbered by counting forward from the first residue of the mature protein (+1, +2, ...) and back into the signal peptide from the first residue upstream of the cleavage site (−1, −2, ...). All results pertaining to "wild type" in this paper refer to a wild-type protein coded for by the WT-Afl gene. (B) The amino acid sequences of the synthetic peptide series are shown amino to carboxyl termini. The wild-type signal peptide of alkaline phosphatase is abbreviated WT. The hydrophobic core regions are highlighted in bold and the amidated carboxyl terminus is designated by the -NH_2 attached to the cysteine. In the corresponding mutant series, the same peptide sequences (lacking the cysteine) serve as signal peptides for alkaline phosphatase; the final alanine of each would then be followed by the first residue of the mature protein, an arginine.

regions, containing different proportions of leucine and alanine residues, represent functional and nonfunctional mutant core regions as determined by a previous study in an otherwise wild-type signal peptide (Doud et al., 1993). The same cleavage region was used in all idealized sequences: alanine was selected for the −1 and −3 positions because it is the most common residue at these signal peptidase recognition sites (von Heijne, 1984). The remainder of the cleavage region is comprised of serine residues; this uncharged amino acid, frequently found throughout native cleavage regions is a polar residue apparently indifferent to formation or disruption of α-helical or β-sheet structures (Chou & Fasman, 1978; Munoz & Serrano, 1994). Studies in our laboratory had already indicated that the presence of helix breaking or β-turn forming residues, such as proline or glycine, are not required for efficient cleavage (Laforet & Kendall, 1991; Jain et al., 1994). Thus, the polyserine sequence provides the clear demarcation in polarity between the hydrophobic core and the cleavage region which may be important for efficient transport. The carboxyl terminus of the synthetic peptides is amidated to avoid introduction of a negative charge which would not be present *in vivo* when attached to the mature protein.

In Vivo Analysis. In order to test the design of the idealized signal sequences, signal peptide mutants of alkaline phosphatase were generated and analyzed for function *in vivo*. Both the 1K7L and 3K7L signal peptide mutants were efficiently processed and transported in *E. coli*, demonstrating that a completely idealized signal peptide which contains only leucines, alanines, and serines in the core and carboxyl regions can be fully functional. Pulse−chase analysis was used to determine the degree of precursor processing at various time intervals (Table 1). These two mutants essentially show complete processing within 30 s, indicating

Table 1: Precursor Processing of Alkaline Phosphatase Signal Peptide Mutants[a]

	Time			
mutant	30 s	1 min	5 min	20 min
WT	87	93	96	96
3K2L	9	6	8	19
1K2L	8	5	6	13
3K7L	97	97	97	96
1K7L	96	97	96	93

[a] The values are expressed as the percent of alkaline phosphatase in the mature form and are the result of the average of two pulse-chase experiments as described in Materials and Methods.

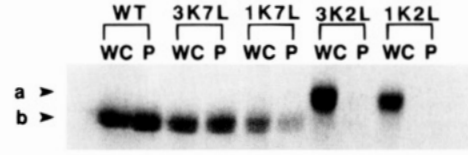

FIGURE 2: Cell fractionation of alkaline phosphatase signal peptide mutants. Cell fractionation was performed as described in Materials and Methods. Arrowheads mark the positions of precursor (a) and mature (b) forms of alkaline phosphatase in whole cell (WC) and periplasmic (P) fractions.

that the multiple positive charges in 3K7L are not required for efficient transport. In fact, both mutants appear to be slightly more efficient than the wild-type signal sequence which at 30 s shows a slight accumulation of precursor that processes over time. Cell fractionation of cells harboring these mutants confirmed the correct localization of the mature enzyme to the periplasmic space (Figure 2). In contrast, the 1K2L and 3K2L mutants are dysfunctional *in vivo* demonstrating the importance of a high leucine to alanine ratio for signal peptide function. Pulse−chase analysis and cell fractionation reveals extensive accumulation of unprocessed precursor with chasing of only ~10% to the periplasmic mature form after 20 min. Any differences in function between the mutants due to the charge variation in the amino terminus are indistinguable by these *in vivo* studies.

Peptide Purification and Analysis. The corresponding signal sequences were synthesized by solid phase chemistry for investigation of physical properties which might be related to the functional differences of the model signal peptides. After synthesis, the signal peptides were cleaved and purified using only reverse-phase HPLC chromatography under isocratic or shallow gradient conditions. We had to avoid purification using a second ion-exchange step because of the aggregation and poor solubility properties of the peptides. Nevertheless, it was concluded that each peptide was homogenous on the basis of both elution from an analytical reverse-phase column and amino acid analysis, and the identity of each peptide was confirmed by mass spectrometry (Table 2). Interestingly, the purified peptides eluted from the C-4 reverse-phase column with retention times that are in good agreement with the intended design (Table 3): the functional signal peptides show similar hydrophobic properties to WT and the nonfunctional peptides are much more hydrophilic.

Signal Peptide Solution Structure by CD. We examined the synthetic peptides by CD in order to determine the secondary structure of each in various solvents, which mimic the range of environments present in biological systems. The CD spectra of the WT and 3K2L in water (Figure 3) show

Table 2: Physical Characterization of Synthetic Peptides

peptide	MH^+ [found (expected)]	amino acid analysis [aa, found (expected)][a]
WT	2359.5 (2359)	A, 2.85 (3); C, 1.00 (1); F, 1.00 (1); I, 0.97 (1); K, 1.90 (2); L, 4.52 (5); M, 1.12 (1); P, 1.91 (2); S, 1.06(1); T, 2.76 (3); V, 1.00 (1); Z, 0.92 (1)
3K2L	2049 (2049)	A, 10.22 (10); C, 1.00 (1); K, 3.19 (3); L, 1.97 (2); M, 0.91(1); S, 3.74 (4); Z, 0.96 (1)
1K2L	2049 (2049)	A, 10.69 (10); C, 0.91 (1); K, 0.95 (1); L, 2.02 (2); M, 0.82 (1); S, 3.61 (4); Z, 3.00 (3)
3K7L	2260 (2260)	A, 5.55 (5); C, 0.96 (1); K, 2.95 (3); L, 6.97 (7); M, 0.76 (1); S, 3.68 (4); Z, 1.00 (1)
1K7L	2260 (2260)	A, 5.40 (5); C, 0.99 (1); K, 1.00 (1); L, 7.05 (7); M, 0.89 (1); S, 3.74 (4); Z, 3.13 (3)

[a] The amino acids, C and M, were detected in their oxidized forms. For these peptides, Z represents only glutamine since there were no glutamic acid residues present.

Table 3: Structural Properties and Calculated Hydrophobicities of Synthetic Wild-Type and Idealized Signal Peptides

	α-helix (%)[a]				hydrophobicity[b]		
peptide	water	1.0 mM SDS	10 mM SDS	40% TFE	von Heijne	Kyte and Doolittle	r.t.[c]
WT	15(RC)	0(β)	34(α)	31(α)	−7.0 (−1.0)	2.8 (1.0)	24.6
1K2L	0(β)	0(β)	0(β)	13(β)	−5.4 (−0.3)	2.2 (0.6)	16.3
3K2L	8(RC)	0(β)	71(α)	53(α)	−5.4 (0.4)	2.2 (0.5)	16.0
1K7L	ND	ND	ND	93(α)	−8.3 (−1.6)	3.2 (1.0)	25.5
3K7L	19(β)	0(β)	26(β)	100(α)	−8.3 (−1.0)	3.2 (1.0)	23.3

[a] Structural properties were determined by the method of Greenfield and Fasman (1969). For 3K7L, the α-helical content was also estimated by the method of Chen et al. (1974). The CD spectra are classified as random coil (RC), α-helix (α) and β-sheet (β) by shape, according to the method of Greenfield and Fasman (1969). ND: 1K7L was not done in these solvents due to poor solubility. [b] The hydropathy scales of von Heijne (1981) and Kyte and Doolittle (1982) were used to determine the mean hydrophobicity per residue for the core region. Values given in parentheses are hydrophobicities of the entire signal peptide. For the von Heijne hydropathy values, high hydrophobicity is designated by a more negative value; for the Kyte and Doolittle hydropathy values, high hydrophobicity is designated by a more positive value. [c] Retention time for elution from a C4 analytical column eluting with 0−60% acetonitrile in 0.1% TFA over 30 min.

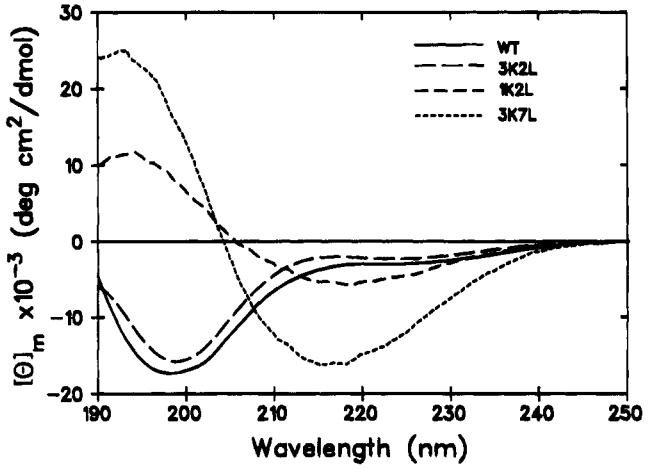

FIGURE 3: CD spectra of peptides in aqueous solution. WT (—), 3K2L (— —), 1K2L (— — —), and 3K7L (- - -) were dissolved to 0.18, 0.21, 0.15, and 0.20 mg/mL and spectra were acquired in 1.0, 1.0, 0.5, and 0.5 mm CD cells, respectively.

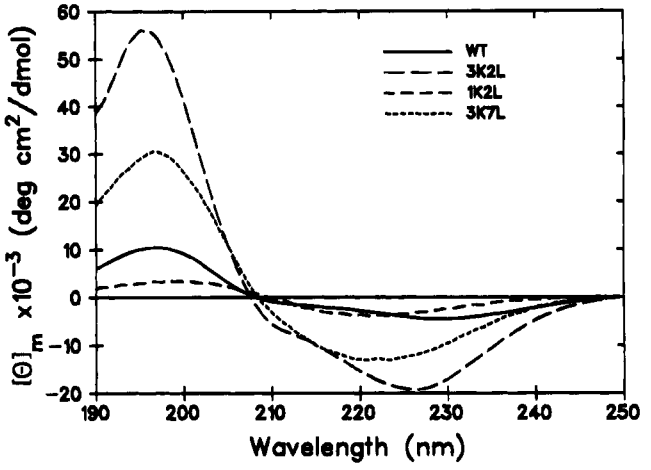

FIGURE 4: CD spectra of peptides in 1.0 mM SDS. WT (—), 3K2L (— —), 1K2L (— — —), and 3K7L (- - -) were dissolved to 0.18, 0.21, 0.15, and 0.20 mg/mL and spectra were acquired in 1.0, 1.0, 0.5, and 0.5 mm CD cells, respectively.

strong minima below 200 nm and a weak shoulder at 225 nm, extrema typical of the $\pi-\pi^*$ and $n-\pi^*$ transitions, respectively, of peptides in a random conformation (Greenfield & Fasman, 1969; Woody, 1985). Analysis of these spectra by the method of Greenfield and Fasman (1969) also suggests that these peptides in water are in mostly nonordered structures, with estimates of 71 and 83% random structure for WT and 3K2L, respectively. These are the only spectra for this peptide series that can be interpreted as containing predominantly random solution conformations.

A second set of CD spectra show characteristics of peptides in β-sheet structures; this series includes 1K2L and 3K7L in water (Figure 3), WT, 1K2L, and 3K7L in 1 mM SDS (Figure 4), and 1K2L in 10 mM SDS (Figure 5). These spectra are relatively symmetrical, with maxima at 193−198 nm and minima at 217−229 nm, extrema expected for the $\pi-\pi^*$ and $n-\pi^*$ transitions, respectively, and with crossover points (i.e., $[\phi]_m = 0$) between 204 and 209 nm, spectral characteristics observed for peptides with β-sheet structure (Greenfield & Fasman, 1969; Woody, 1985). In spite of the apparent similarities in the shape of this series of spectra, they differ in relative intensity. For example, the extrema for 3K7L in water and 1.0 mM SDS are 2−10 times those observed for 1K2L in the same solvents. These intensity differences could be related to differences in the relative proportions of other secondary structures. For example, analysis of the 1K2L spectrum in water gives no α-helical structure, whereas the 3K7L spectrum in water gives 19% α-helical structure (Table 3). Thus, for 3K7L, the increased intensities at 208 nm (as well as at 195 and 222 nm) translate into higher apparent α-helical structure (Greenfield & Fasman, 1969). Alternatively, Woody (1985) suggests that

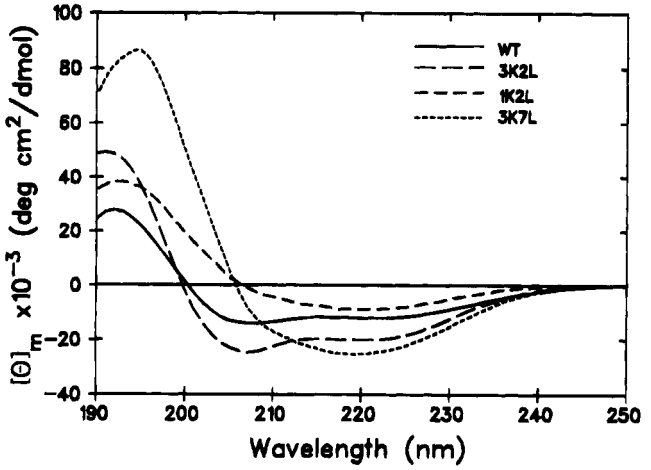

FIGURE 5: CD spectra of peptides in 10 mM SDS. WT (—), 3K2L (— —), 1K2L (— — —), and 3K7L (- - -) were dissolved to 0.18, 0.21, 0.15, and 0.20 mg/mL and spectra were acquired in 1.0, 1.0, 0.5, and 0.5 mm CD cells, respectively.

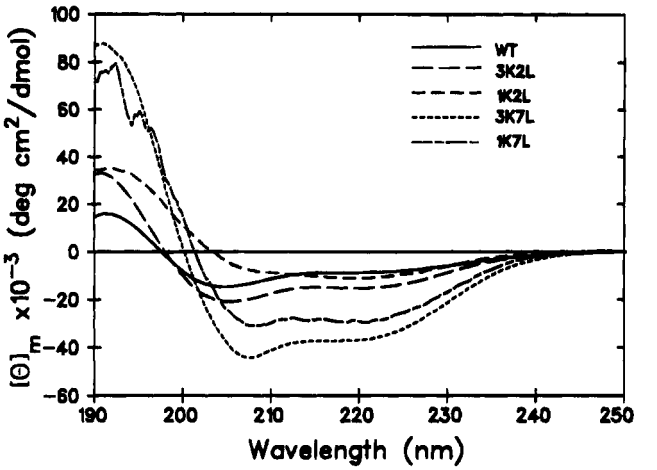

FIGURE 6: CD spectra of peptides in 40% Trifluoroethanol. WT (—), 3K2L (— —), 1K2L (— — —), 3K7L (- - -), and 1K7L (— - — -) were dissolved to 0.18, 0.21, 0.15, 0.20, and 0.07 mg/mL, and spectra were acquired in 1.0, 1.0, 0.5, 0.5, and 0.5 mm CD cells, respectively.

the variability in intensity between the β-sheet-like CD spectra of peptides can be explained based on the orientation, length, width, and twist of the various β-sheet structures. Indeed, there are differences in the film β-sheet structure of polyalanine and polyleucine heptamers, with polyalanine forming predominantly antiparallel β-pleated sheets (Balcerski et al., 1976) and polyleucine forming a combination of both parallel and antiparallel β-sheets (Kelly et al., 1977). Therefore, the observed intensity differences can be easily explained as differences in global β-sheet structure resulting from differences in the amino acid content of the core regions.

The spectral shape of 3K7L in 10 mM SDS (Figure 5) has characteristics of both β-sheet and α-helical structures. This spectrum has a strong shoulder at 209 nm, a strong minimum at 220 nm, and a strong maximum at 194 nm, features consistent with the spectrum of an α-helical structure, but it lacks the distinct minimum at 209 nm and has a crossover point at 205 nm, features characteristic of a β-sheet-like spectrum (Greenfield & Fasman, 1969; Woody, 1985). A direct comparison between the spectra of 3K7L in 1.0 and 10 mM SDS gives a good method for determining the origin of the increased intensities of the spectrum in 10 mM SDS. Relative to the spectrum in 1.0 mM SDS, the spectrum in 10 mM SDS exhibits lower ellipticity at 209 and 222 nm by 13 500 and 11 000 deg cm^2/dmol, respectively, and has a stronger maximum at 194 nm (shifted from 197 nm) with an increased intensity of 56 000 deg cm^2/dmol. Thus, for 3K7L, the difference between the spectra in 10 and 1.0 mM SDS yields a spectrum with features characteristic of an α-helix, indicating an induction of about 29% α-helical structure in 10 mM SDS based on the difference in intensity at 208 as calculated by the method of Greenfield and Fasman (1969). Interestingly, the spectrum of 3K7L does not change further with incremental increases in SDS concentration up to 300 mM, nor does the spectrum change with incremental temperature increases from 25 to 70 °C (data not shown).

The third set of CD spectra are characteristic of those expected from peptides in an α-helical conformation; this set includes the CD spectra of 3K2L and WT in 10 mM SDS (Figure 5) and all peptides in 20% (data not shown) and 40% TFE (Figure 6). These spectra show strong maxima near 195 nm and strong minima near 205−209 nm, characteristic of the exciton splitting of the $\pi-\pi^*$ transitions observed in the CD spectra of peptides with α-helical structure, and minima or shoulders at >220 nm, characteristic of the $n-\pi^*$ transitions (Greenfield & Fasman, 1969; Woody, 1985). However, these α-helical-like CD spectra vary considerably in relative intensity, probably reflecting differences in α-helix content (Greenfield & Fasman, 1969). In the case of WT and 3K2L, peptides with random structure in aqueous solution, the spectra in 40% TFE and 10 mM SDS are similar in shape, but with estimated helical contents of 31 and 34%, respectively, for WT, and 53 and 71%, respectively for 3K2L (Table 3). Further analysis of the WT and 3K2L spectra in 40% TFE indicates that the remainder of the structure is accounted for by random coil. In addition, of the five peptides in this series, only WT and 3K2L show isodichroic points in going from 0 to 40% TFE (data not shown), evidence suggesting a simple two-state transition in the titrations.

The α-helical CD spectra of both 1K7L and 3K7L in 40% TFE, with $[\phi]_{222} = -32\,000$ and $-36\,250$ deg cm^2/dmol, respectively, are indicative of high helical content (Figure 6). Analysis of the 1K7L and 3K7L CD spectra in 40% TFE yields estimates of approximately 93 and 100% α-helical content, respectively. Because the $[\phi]_{208}$ for the 3K7L spectrum is greater than the intensity of the Greenfield and Fasman reference spectra, we also calculated the helical contents from $[\phi]_{222}$ by the method of Chen et al. (1974), which also yields an estimate of 100% α-helical character for 3K7L (the value of $[\phi]_{222}$ for 3K7L is, within experimental error, identical to that expected for a 22 amino acid α-helical peptide). In contrast to the random to α-helical structural equilibrium for WT and 3K2L, the absence of isodichroic points in the TFE titrations of 1K7L and 3K7L is further evidence that these peptides undergo a transition from an aggregated β-sheet structure in water to an α- helix in TFE (Batenburg et al., 1988).

In summary, for those peptides with predominantly random structure in water, WT and 3K2L, both TFE and SDS shift the structural equilibrium to include a significant population of α-helical structure. In contrast, for 3K7L, the structure-inducing effects of SDS and TFE are different; the CD

spectra of this peptide in water, 1 and 10 mM SDS reveals mainly β-structure, but in TFE the spectral characteristics of an α-helix are observed. This structural transition suggests that TFE permits disruption of multistranded β-sheets, allowing the observation of the intrinsic α-helical potential of the monomeric state of this highly hydrophobic peptide. Several studies have demonstrated that TFE is a good solvent for differentiating the relative helical potential of isolated peptides (Dyson et al., 1992; Zhong & Johnson, 1992). Thus, analysis of the CD spectra in 40% TFE allows a comparison of the α-helical contents of all five peptides in the series (Table 3). Interestingly, the most efficient peptides *in vivo*, 1K7L and 3K7L, display unusually high α-helical contents, 93 and 100%, respectively, whereas, the nonfunctional signal peptides, 1K2L and 3K2L, exhibit α-helical propensities above and below that determined for the WT signal sequence, 31%. This illustrates a significant difference in the helical propensities of the two core regions in the structure-promoting solvent, TFE, which, in turn, suggests a difference in the helical propensities of the component residues, leucine and alanine, in the context of a signal peptide.

DISCUSSION

In earlier studies, we prepared a series of mutant signal sequences in which the hydrophobicity of the core region was increased by changing the ratios of leucine to alanine from 0:10 to 10:0 (Doud et al., 1993). Using precursor processing as a measure of transport efficiency, we demonstrated a sigmoidal relationship between transport and core segment hydrophobicity, with a minimum hydrophobicity level characterized by leucine to alanine ratios of 4:6 or 5:5 required for efficient transport. In the present study, we prepared fully idealized signal sequence mutants with core regions on each side of this minimum hydrophobicity requirement. The core regions of these signal sequences contain leucine and alanine in ratios of 7:3 and 2:8, representing functional and nonfunctional core regions, respectively. Additionally, we synthesized the corresponding signal peptides and characterized them for solution conformational preferences. The functional signal sequences, i.e., those with leucine to alanine ratios of 7:3, show a strong preference for α-helical structure in TFE, a structure-promoting solvent, whereas one nonfunctional sequence, 1K2L, shows a β-sheet preference essentially independent of solvent, while a second nonfunctional sequence, 3K2L, shows a moderate preference for an α-helical structure. Thus, the *in vivo* function of the idealized signal sequences shows a strong correlation with both hydrophobicity and α-helical propensity of the signal peptide.

A useful measure of the hydrophobicity of these signal sequences is the relative retention time of the corresponding synthetic signal peptides for elution from reverse-phase HPLC. The lysine to glutamine conversions in the amino-terminal region shift the retention time to slightly longer time periods, regardless of the core region, as might be expected for the decrease in positive charge. However, the more dramatic effect is between the retention times of the peptides with two leucines in the core region versus those with seven leucines. These HPLC retention times correlate with the calculated hydrophobicities of both the signal sequence core and the entire signal peptide using the hydrophobicity scales of von Heijne (1981) and Kyte and Doolittle (1982) (Table 3). The functional signal sequences were designed to have hydrophobicity characteristics similar to those of the wild-type sequence. Thus, the intermediate HPLC retention time of the WT signal peptide relative to that of the 7L signal sequences illustrates the accuracy of our design.

In addition to their strong hydrophobicity, the core regions of the functional signal sequences (i.e., 1K7L and 3K7L) also show a strong tendency to form and propagate α-helical structure in a structure-promoting solvent. The strong helical preferences of 1K7L and 3K7L in aqueous TFE are due to the helical content of the core segment since the nonfunctional sequences, which differ in the core region but have identical amino- and carboxyl-terminal regions, lack this helical potential. The strong intensities of the α-helical-like CD spectra of 1K7L and 3K7L are unusual but have been observed in other systems (Holzwarth & Doty, 1965; Townend et al., 1966; Chen et al., 1974). Recently, Su et al. (1994) designed amphiphilic peptides with salt bridges included to stabilize the helix ends. Although 3K7L and 1K7L lack such stabilizing bridges, their CD spectra in 40% TFE are nearly identical to the CD spectra of these highly helical model peptides in 50% TFE. Apparently, the core region of 3K7L and 1K7L propagates the helical structure into the hydrophilic region of both the amino and carboxyl termini.

Chou−Fasman analysis (Chou & Fasman, 1978) of natural signal sequences predicts both α-helix and β-sheet structures (Austen, 1979; Rosenblatt et al., 1980), and CD spectra of wild-type synthetic peptides often reveal both structures in a solvent-dependent manner (Gierasch, 1989). For example, the PhoE signal peptide is induced into an α-helical structure by anionic phospholipids and SDS micelles but maintains partial to full β-sheet structure in cardiolipin and zwitterionic vesicles (Batenburg et al., 1988; Keller et al., 1992). Although we were unable to quantitatively investigate the structural properties of 1K7L in aqueous and SDS solutions, the spectra of 3K7L in water and 1.0 mM SDS (i.e., below the critical micelle concentration) are similar to the β-sheet-like CD spectra of the synthetic wild-type signal sequences of PhoE (Batenburg et al., 1988; Keller et al., 1992), OmpA (Hoyt & Gierasch, 1991) and preproparathyroid hormone (Rosenblatt et al., 1980). However, β-structures often involve the formation of multistranded sheets and, thus, may not be relevant to the *in vivo* activity of signal peptides.

The structural properties of the nonfunctional sequences 1K2L and 3K2L show differences not only compared to the functional peptides but also show striking differences between themselves which can only be related to the sequence differences in the amino-terminal region. Peptide 1K2L maintains β-sheet-like structure in water and 1.0 and 10 mM SDS and shows only a small induction of α-helical structure in 40% TFE. In contrast, 3K2L shows random structure in water and maintains a random to α-helix equilibrium in SDS and TFE. Thus, the lysine and glutamine residues in the amino terminus exert diverse end effects on the apparently flexible structure of the alanine and serine polymer.

The calculated 53% α-helical structure of the nonfunctional 3K2L in 40% TFE is within the range of values for α-helicity (46−62%) of several wild-type peptides under similar conditions and calculated by similar methods (Rosenblatt et al., 1980; Batenburg et al., 1988; Bruch & Gierasch, 1990; Rizo et al., 1993). In contrast, the 31% α-helical

structure of the WT peptide is significantly lower than that of the nonfunctional 3K2L. The structural potential of 3K2L in aqueous solution with TFE and SDS cosolvents relative to WT and other synthetic wild type signal sequences confirms that α-helicity in the absence of strong hydrophobicity is not sufficient to support transport (McKnight et al., 1989; Hoyt & Gierasch, 1991). However, the lower, yet significant, structural potential of WT is explained by the presence of two prolines at position −5 and −10 in the signal sequence, helix-breaking residues which are absent from the idealized signal sequence 3K2L. These proline residues in the WT break up the helical structure of the core, preventing propagation of the helix through the core and into the cleavage site and limiting the helical potential of this peptide in solution.

Many other natural signal sequences contain a helix-breaking residue such as proline or glycine upstream from the cleavage site, but the role of this residue remains an unresolved issue. Yamamoto et al. (1990) designed simplified artificial signal sequences which revealed that changing proline at the −11 position to leucine significantly increases signal peptide helicity but severely decreases export activity. Yamamoto proposed a model for signal peptide function in which a proline residue carboxyl-terminal to the core allowed the sequence in the cleavage region to unfold from an α-helical structure for (or during) interaction with the signal peptidase. However, our results with the idealized signal sequences suggest a second, complementary explanation for these helix-breaker residues. In 3K7L and 1K7L, the idealized core region has a high hydrophobicity as well as strong helical structure that extends into both termini, but the idealized cleavage sequence is hydrophilic, providing a clear hydrophobic-hydrophilic boundary between these two regions. In the presence of this definitive boundary, the signal peptidase recognizes the cleavage region, despite the absence of a helix-breaker, as evidenced by the fast processing rate of the idealized signal sequences even relative to the wild type. In the study of Yamamoto et al. (1990), replacing the proline at position −11 with leucine might extend the hydrophobic core and abolish the clear border between the core and the cleavage site, causing the signal peptidase to look further downstream for a cleavage site. In natural signal sequences, the proline residue might enhance signal peptidase recognition by causing a kink or local unwinding both of which would expose the polar backbone amide bonds and increase the hydrophilicity of this segment. Thus, the kink or local unwinding of an α-helical segment would provide a clear core-cleavage site boundary similar to that provided by multiple amino acids with hydrophilic side chains.

One advantage of the idealized approach to elucidating signal peptide function is that we can compare the structural properties of the synthetic functional and nonfunctional signal sequences without the additional complexities of sequences composed of many different amino acids. Our results with 1K7L and 3K7L suggest that the functional signal sequence is characterized by a highly hydrophobic core region with strong α-helical potential. Although the amino acids used in both the functional and nonfunctional core regions show similar statistical and theoretical preferences for α-helical structures in both proteins and soluble peptides (Lyu et al., 1990; O'Neil & DeGrado, 1990; Padmanabhan et al., 1990; Creamer & Rose, 1992), this high helical potential is absent or modest in the polyalanine-containing nonfunctional signal peptides in comparison to the polyleucine-containing sequences in TFE. This difference in the structural properties of the two core regions suggests a difference in the α-helical propensity of leucine and alanine at least in the context of idealized signal peptides. Although we cannot conclude to what extent the data in TFE reflect the intrinsic structural propensities, the apparent difference between the leucine and alanine is consistent with the statistical evaluation of helices when boundary residues are omitted (Chou & Fasman, 1974). The analysis by Chou and Fasman revealed a higher occurrence of leucines as compared to alanines in internal positions of helices, suggesting a potential for leucine to nucleate as well as stabilize helical segments. The different propensities observed in our series may be magnified by the presence of multiple leucines within the core of the signal sequence, effectively nucleating and propagating the helix throughout the peptide. It is also reasonable that other studies, which examined the effect of only one or a few guest residues on the stability of a host helical segment, might not reveal the same rank order of residues.

This difference in helical propensity, in turn, sheds light on previous studies involving signal peptide mutants containing core regions composed of varying ratios of these two residues (Rusch et al., 1994). We showed that core region mutants containing extremely high ratios of leucine to alanine, 9:1 and 10:0, function efficiently yet, by some criteria, are different compared to functional sequences with lower ratios of leucine to alanine residues; the 9L1A and 10L0A mutants are insensitive to transport inhibitors such as sodium azide and CCCP and show substantial inhibition of processing of the co-expressed wild-type precursor β-lactamase. We suggested that these core regions have an unusually high affinity for a secretory component such as SecA; this affinity was attributed only to hydrophobicity because the α-helicity was assumed to be very similar. Yet the present study suggests that α-helicity, as well as high hydrophobicity, may play a key role in utilizing the secretory pathway.

REFERENCES

Akita, M., Sasaki, S., Matsuyama, S., & Mizushima, S. (1990) *J. Biol. Chem. 265*, 8164−8169.

Austen, B. M. (1979) *FEBS Lett. 103*, 308−313.

Balcerski, J. S., Pysh, E. S., Bonora, G. M., & Toniolo, C. (1976) *J. Am. Chem. Soc. 98*, 3470−3473.

Batenburg, A. M., Brasseur, R., Ruysschaert, J.-M., van Scharrenburg, G. J. M., Slotboom, A. J., Demel, R. A., & de Kruijff, B. (1988) *J. Biol. Chem. 263*, 4202−4207.

Bruch, M. D., & Gierasch, L. M. (1990) *J. Biol. Chem. 265*, 3851−3858.

Chen, Y.-H., Yang, J. T., & Chau, K. H. (1974) *Biochemistry 13*, 3350−3359.

Chou, P. Y., & Fasman, G. D. (1974) *Biochemistry 13*, 211−222.

Chou, P. Y., & Fasman, G. D. (1978) *Annu. Rev. Biochem. 47*, 251−276.

Creamer, T. P., & Rose, G. D. (1992) *Proc. Natl. Acad. Sci. U.S.A. 89*, 5937−5941.

de Vrije, T., Batenburg, A. M., Killian, J. A., & de Kruijff, B. (1990) *Mol. Microbiol. 4*, 143−150.

Doud, S. K., Chou, M. M., & Kendall, D. A. (1993) *Biochemistry 32*, 1251−1256.

Dyson, H. J., Sayre, J. R., Merutka, G., Shin, H.-C., Lerner, R. A., & Wright, P. E. (1992) *J. Mol. Biol. 226*, 819−835.

Forood, B., Feliciano, E. J., & Nambiar, K. P. (1993) *Proc. Natl. Acad. Sci. U.S.A. 90*, 838−842.

Gierasch, L. M. (1989) *Biochemistry 28*, 923−930.

Greenfield, N., & Fasman, G. D. (1969) *Biochemistry 8*, 4108−4116.
Holzwarth, G., & Doty, P. (1965) *J. Am. Chem. Soc. 87*, 218−226.
Hoyt, D. W., & Gierasch, L. M. (1991) *Biochemistry 30*, 10155−10163.
Jain, R. G., Rusch, S. L., & Kendall, D. A. (1994) *J. Biol. Chem. 269*, 16305−16310.
Keller, R. C. A., Killian, J. A., & de Kruijff, B. (1992) *Biochemistry 31*, 1672−1677.
Kelly, M. M., Pysh, E. S., Bonora, G. M., & Toniolo, C. (1977) *J. Am. Chem. Soc. 99*, 3264−3266.
Kendall, D. A., Bock, S. C., & Kaiser, E. T. (1986) *Nature 321*, 706−708.
Kyte, J., & Doolittle, R. F. (1982) *J. Mol. Biol. 157*, 105−132.
Laemmli, U. K. (1970) *Nature 227*, 680−685.
Laforet, G. A., & Kendall, D. A. (1991) *J. Biol. Chem. 266*, 1326−1334.
Lyu, P. C., Liff, M. I., Marky, L. A., & Kallenbach, N. R. (1990) *Science 250*, 669−673.
McKnight, C. J., Briggs, M. S., & Gierasch, L. M. (1989) *J. Biol. Chem. 264*, 17293−17297.
Miller, J. H. (1972) *Experiments in Molecular Genetics*, Cold Spring Harbor Laboratory, Cold Spring Harbor, NY.
Moore, S., & Stein, W. H. (1954) *J. Biol. Chem. 211*, 907−913.
Munoz, V., & Serrano, L. (1994) *Proteins: Struct., Funct., Genet. 20*, 301−311.
Neidhardt, F. C., Bloch, P. L., & Smith, D. F. (1974) *J. Bacteriol. 119*, 736−747.
O'Neil, K. T., & DeGrado, W. F. (1990) *Science 250*, 646−650.
Padmanabhan, S., Marqusee, S., Ridgeway, T., Laue, T. M., & Baldwin, R. L. (1990) *Nature 344*, 268−270.
Park, S., Liu, G., Topping, T. B., Cover, W. H., & Randall, L. L. (1988) *Science 239*, 1033−1035.
Puziss, J. W., Fikes, J. D., & Bassford, P. J., Jr. (1989) *J. Bacteriol. 171*, 2303−2311.
Randall, L. L., & Hardy, S. J. S. (1986) *Cell 46*, 921−928.
Rizo, J., Blanco, F. J., Kobe, B., Bruch, M. D., & Gierasch, L. M. (1993) *Biochemistry 32*, 4881−4894.
Rosenblatt, M., Beaudette, N. V., & Fasman, G. D. (1980) *Proc. Natl. Acad. Sci. U.S.A. 77*, 3983−3987.
Rusch, S. L., Chen, H., Izard, J. W., & Kendall, D. A. (1994) *J. Cell. Biochem. 55*, 209−217.
Sanger, F., Nicklen, S., & Coulson, A. R. (1977) *Proc. Natl. Acad. Sci. U.S.A. 74*, 5463−5467.
Su, J. Y., Hodges, R. S., & Kay, C. M. (1994) *Biochemistry 33*, 15501−15510.
Townend, R., Kumosinski, T. F., Timasheff, S. N., Fasman, G. D., & Davidson, B. (1966) *Biochem. Biophys. Res. Commun. 23*, 163−169.
von Heijne, G. (1981) *Eur. J. Biochem. 116*, 419−422.
von Heijne, G. (1984) *J. Mol. Biol. 173*, 243−251.
Woody, R. W. (1985) in *The Peptides* (Hruby, V. J., Ed.) pp 15−114, Academic Press, Orlando, FL.
Yamamoto, Y., Ohkubo, T., Kohara, A., Tanaka, T., Tanaka, T., & Kikuchi, M. (1990) *Biochemistry 29*, 8998−9006.
Zhong, L., & Johnson, W. C., Jr. (1992) *Proc. Natl. Acad. Sci. U.S.A. 89*, 4462−4465.

BI950656I